Biophysical Journal, Volume *112*

Supplemental Information

Small-Volume Effect Enables Robust, Sensitive, and Efficient Information Transfer in the Spine

Masashi Fujii, Kaoru Ohashi, Yasuaki Karasawa, Minori Hikichi, and Shinya Kuroda

Supplement to “Small-volume effect enables robust, sensitive and efficient information transfer in the spine”

Masashi Fujii,[1,2] Kaoru Ohashi,[1] Yasuaki Karasawa,[3] Minori Hikichi,[1] and Shinya Kuroda [1,2,4,*]

[1]Molecular Genetics Research Laboratory, Graduate School of Sciences, University of Tokyo, Bunkyo-ku, Tokyo, Japan
[2]Department of Biological Sciences, Graduate School of Sciences, University of Tokyo, Bunkyo-ku, Tokyo, Japan
[3]Department of Neurosurgery, Graduate School of Medicine, University of Tokyo, Bunkyo-ku, Tokyo, Japan
[4]CREST, Japan Science and Technology Agency, Bunkyo-ku, Tokyo, Japan

[*]Corresponding author
E-mail: skuroda@bs.s.u-tokyo.ac.jp (SK)

Supporting Material Figures

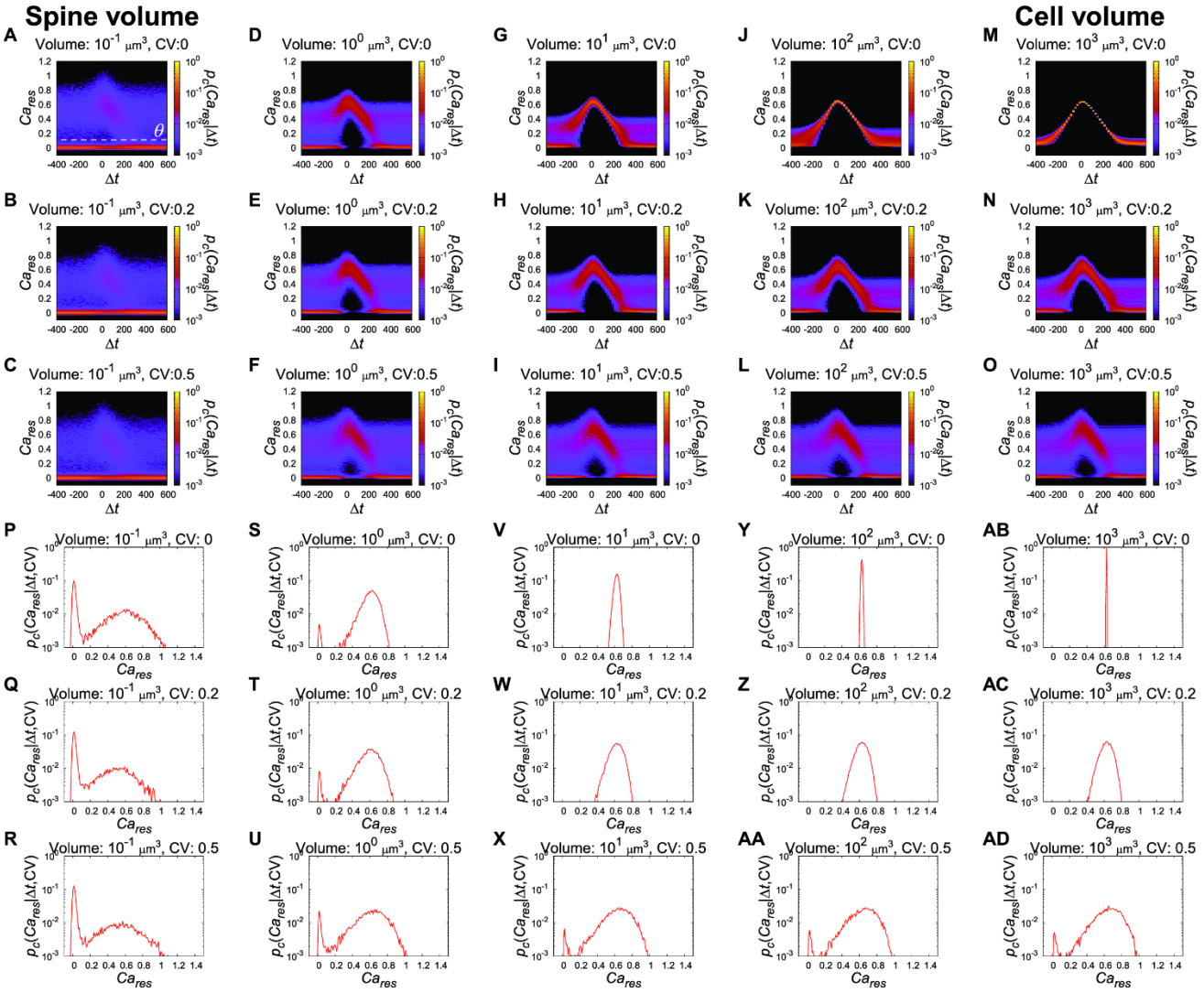

Figure S1. The Δt-dependency of the distribution of Ca_{res}. (*A–O*) The volume and CV of the amplitude of PF input are indicated. In the spine volume, the distribution of Ca_{res} is divided into two distributions by the threshold θ =0.157 defined as the local minimum of the marginal distribution of Ca_{res} for Δt *s.t.* $p_c(Ca_{res}) = \int_{\Delta t} p_{in}(\tau) p_c(Ca_{res}|\tau)\, d\tau$. (*P–AD*) The cross-sections of (*A–O*) with $\Delta t = 0$. This distribution of Ca_{res} in the spine volume remained the same regardless of the CV_a value, whereas, that in the cell volume largely varied.

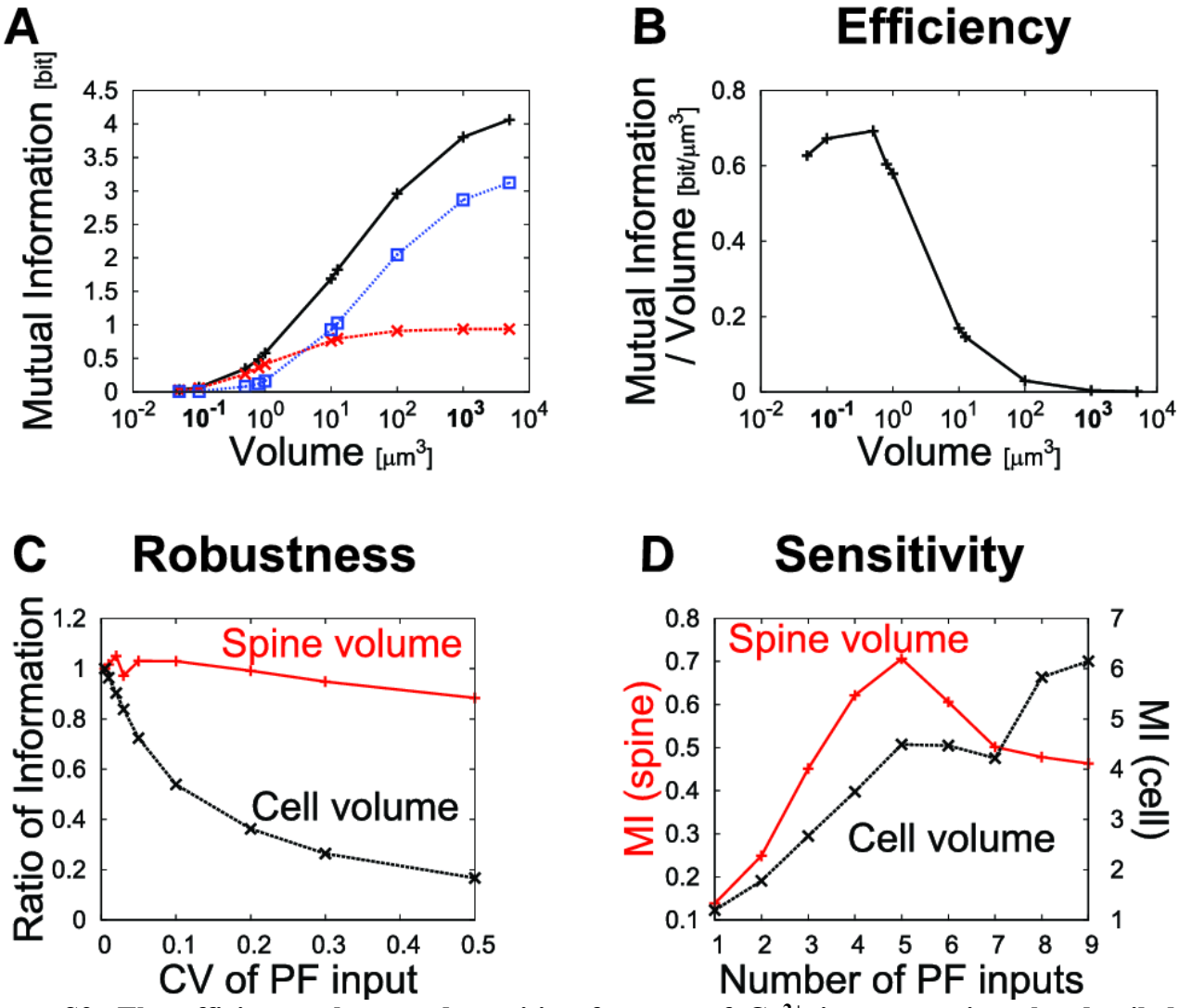

Figure S2. The efficient, robust and sensitive features of Ca^{2+} increase using the detailed stochastic model (23)**.** (*A*) The volume dependency of the mutual information between Δt, the PF- and CF-timing, and Ca_{res}, Ca^{2+} response. Total mutual information is indicated in *black*; that of the probability component is indicated in *red*; that of the amplitude component is indicated in *blue*. (*B*) The volume dependency of the mutual information per volume. (*C*) The CV of the amplitude of PF input dependency of the mutual information. (*D*) The number of PF inputs dependency of the mutual information. In the detailed stochastic model, the spine volume is 10^{-1} μm^3 and the cell volume is 5×10^3 μm^3 (23)

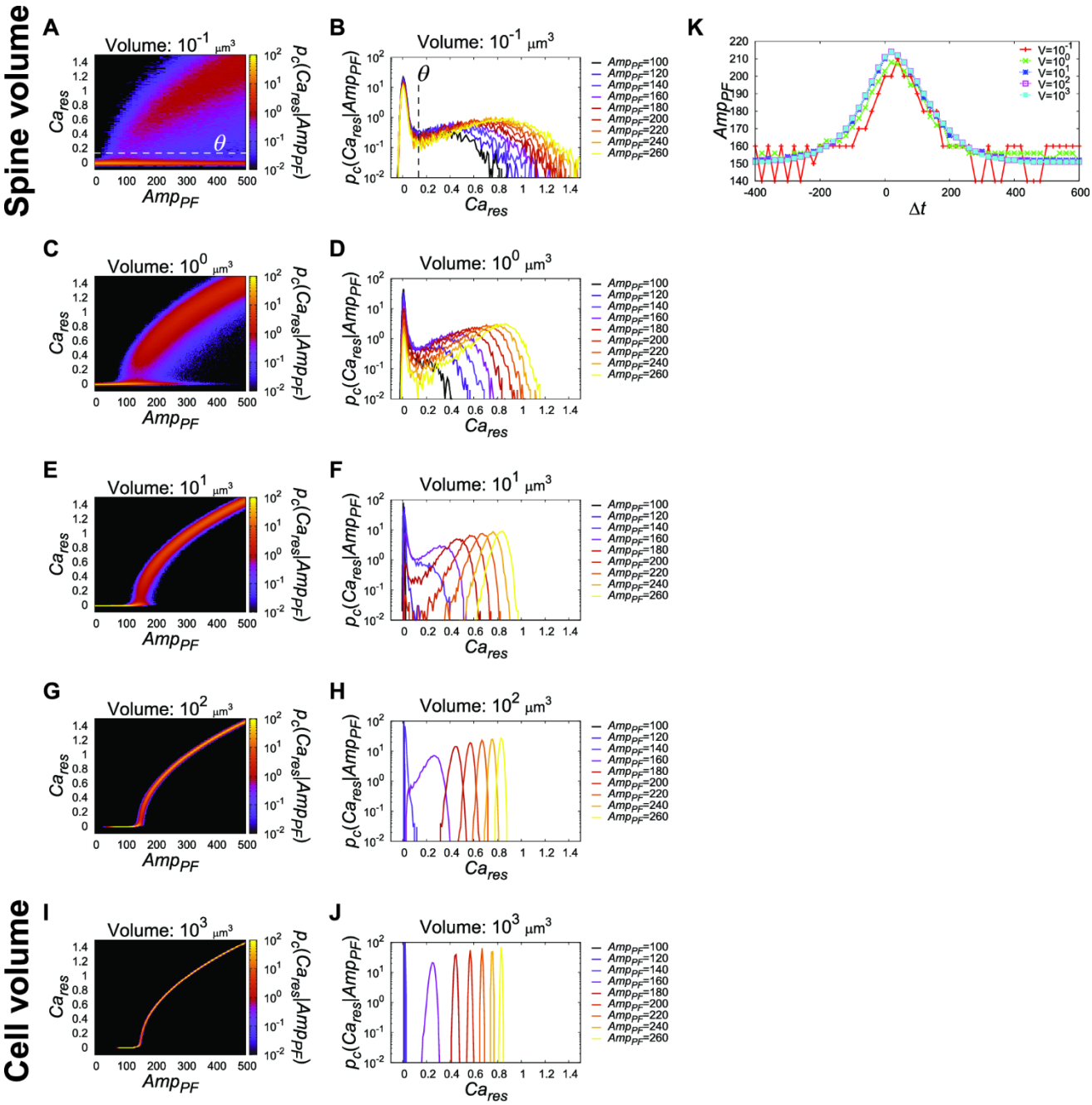

Figure S3. The Amp_{PF}-dependency of the distribution of Ca_{res} in the indicated volumes. (*A*, *C*, *E*, *G*, *I*) Distribution of Ca_{res}. (*B*, *D*, *F*, *H*, *J*) The cross-section of distribution of Ca_{res} at the indicated Amp_{PF}. $\theta(=0.157)$ indicates the threshold dividing the distribution into the ranges with large Ca_{res} and with small Ca_{res} (see Fig. S1). (*K*) The Amp_{PF} providing $p_c(Ca_{res}|Amp_{PF})$, the distribution of Ca_{res} with PF input alone, closest to $p_c(Ca_{res}|\Delta t)$, the distribution of Ca_{res} with PF and CF inputs with various Δt.

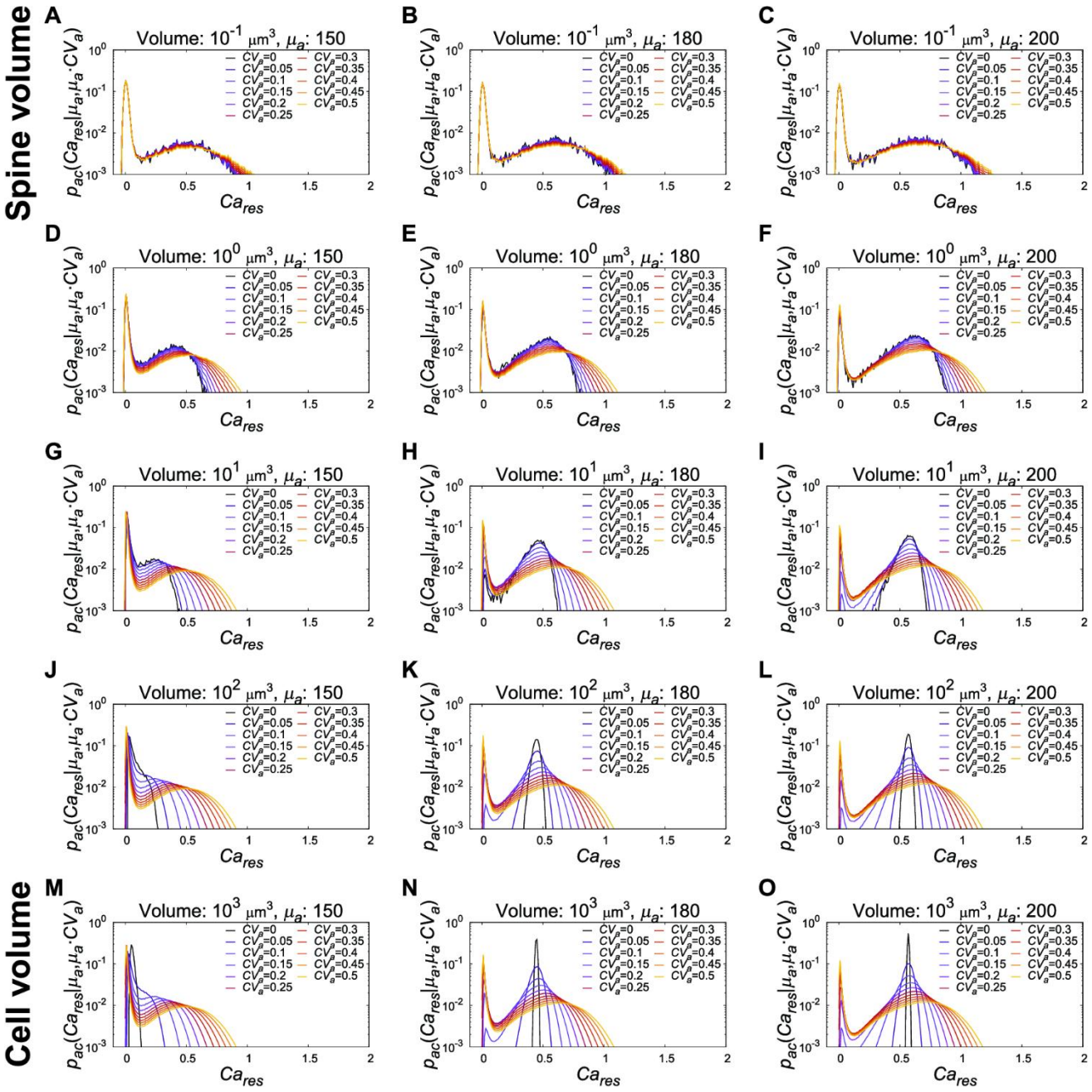

Figure S4. Distributions of Ca_{res} against CV_a with the indicated volumes and μ_a, the average of Amp_{PF}.

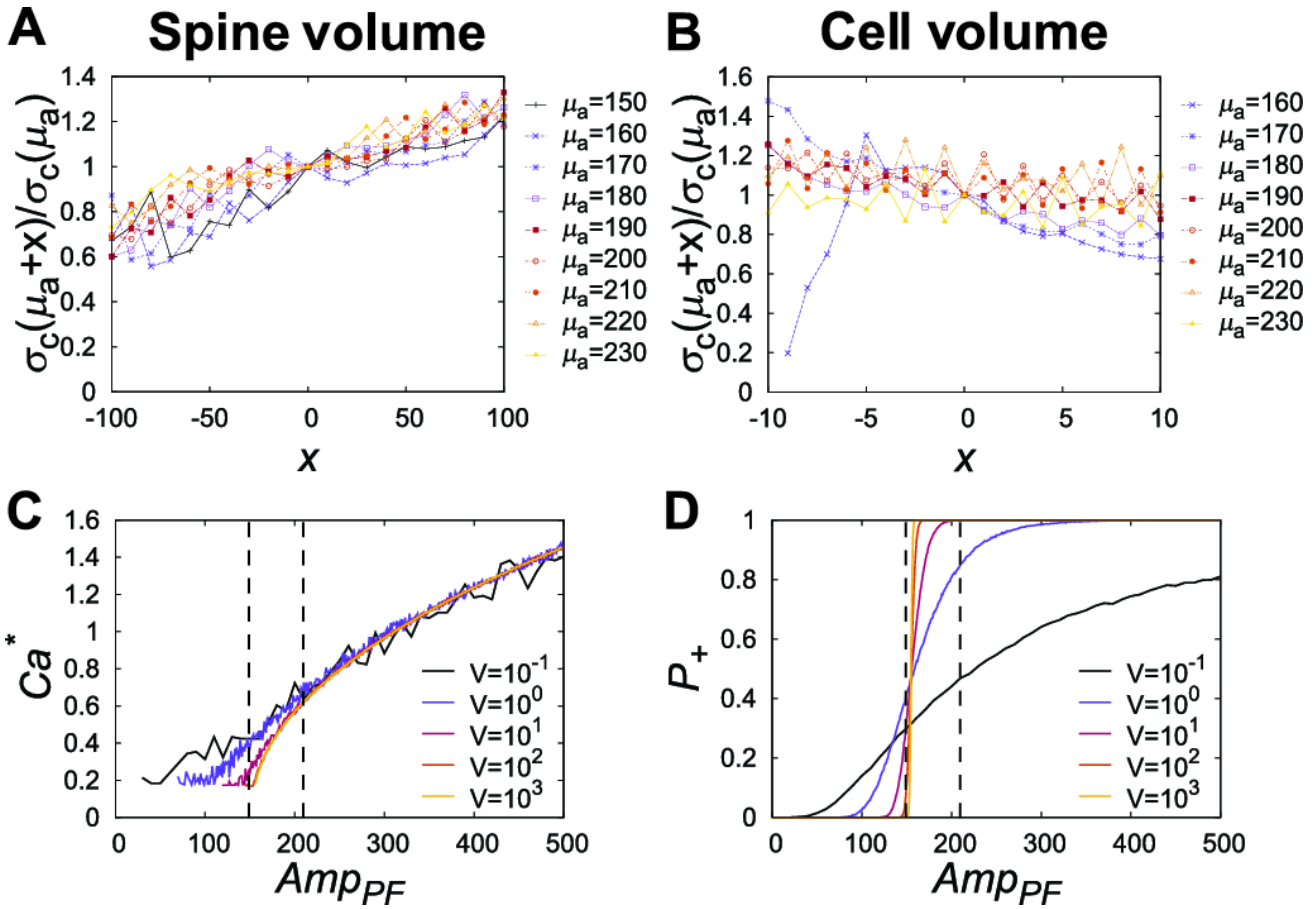

Figure S5. The Amp_{PF} dependency of σ_c, Ca^* and P_+. (*A*, *B*) $\sigma_c(\mu_a + x)$ can be regarded as $\sigma_c(\mu_a)$ up to the upper bound of the range of x satisfying the Eq. 21 in the main text. (*A*) Spine volume. (*B*) Cell volume. $\sigma_c(\mu_a + x)/\sigma_c(\mu_a)$ were almost within the range of 0.8 to 1.2, assuming that $\sigma_c(\mu_a + x)$ is approximated by $\sigma_c(\mu_a)$. The upper bound of the range of x satisfying Eq. 21 in the main text in the spine and cell volumes are determined by $\delta_{\max}$ (see Fig. 4*A*, *B*). (*C*) The Amp_{PF}-dependency of Ca^*, the mode of the distribution of Ca_{res} for $Ca_{res} > \theta$. (*D*) The Amp_{PF}-dependency of P_+, the probability of $Ca_{res} > \theta$.

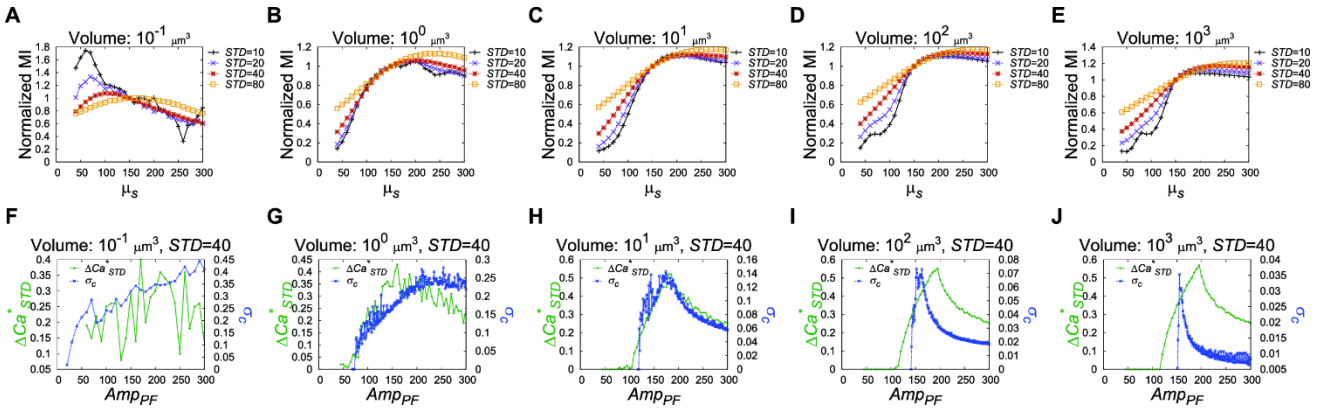

Figure S6. Mechanism of the sensitivity. (*A–E*) μ_s, the average of the input distribution of Amp_{PF}, dependency of the mutual information normalized by the value of that with $Amp_{PF} = 150$. (*F–J*) The Amp_{PF} dependencies of ΔCa^*_{STD}, the dynamic range of the distribution of Ca_{res}, (*green*) and σ_c, the standard deviation of Ca_{res}, (*blue*) for $Ca_{res} > \theta$. The volume is indicated.

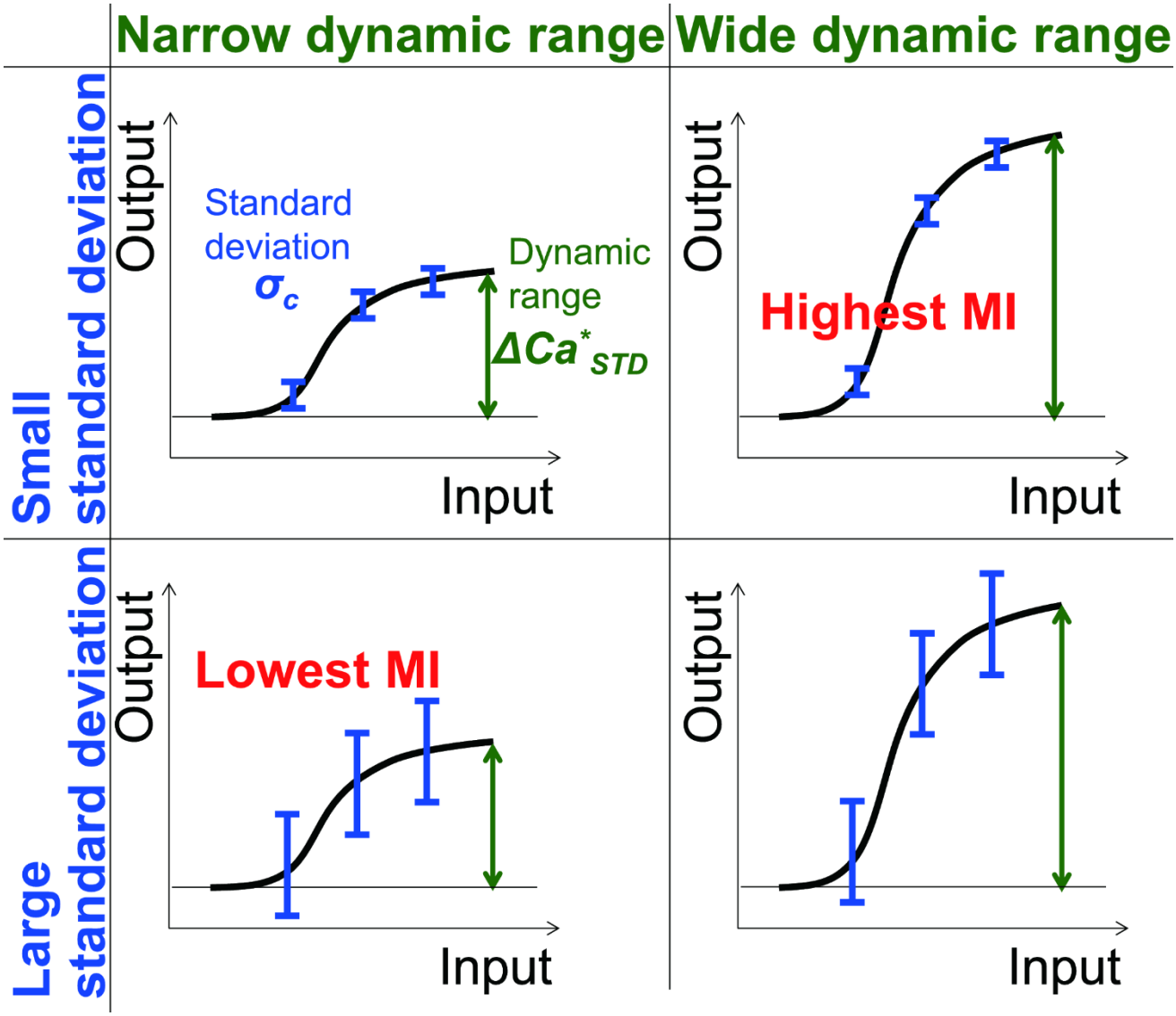

Figure S7. The mutual information depends on both ΔCa^*_{STD}, the dynamic range, and σ_c, the standard deviation of the distribution of the output. In general, if the input distribution is the same, then the wider ΔCa^*_{STD}, the dynamic range of the output, gives more mutual information when σ_c, the standard deviation of the output, is the same (compare the *left* and *right* panels). The smaller σ_c gives more mutual information when ΔCa^*_{STD} is the same (compare the *top* and *bottom* panels).

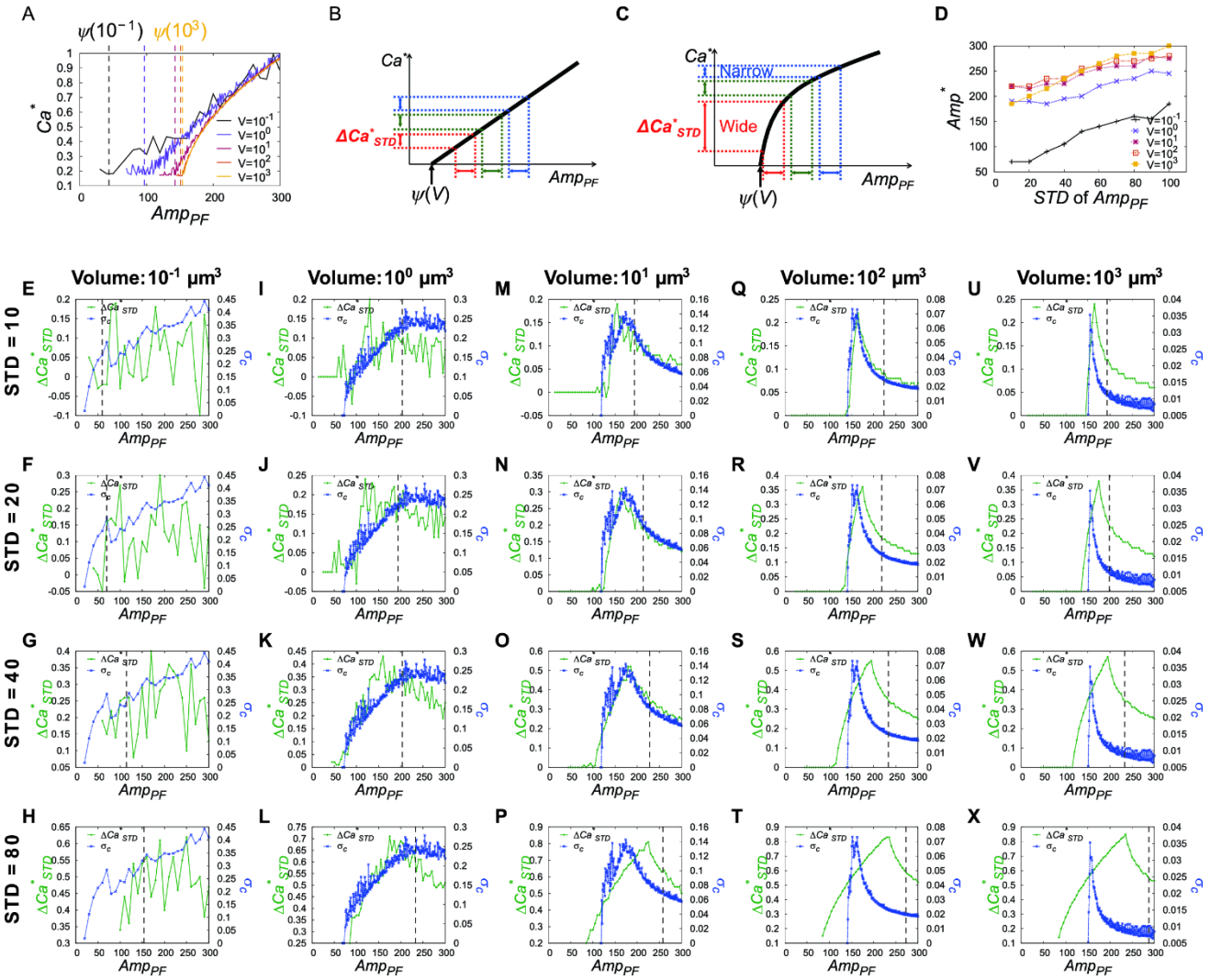

Figure S8. ΔCa^*_{STD}, the dynamic range, and σ_c, the standard deviation of the distribution of the output. (*A*) The Amp_{PF} dependency of Ca^*, the mode of the distribution of Ca_{res} for $Ca_{res} > \theta$. We defined $\psi(V)$ for each volume of the Amp_{PF} when the Ca^* began to increase. In the spine volume, $\psi(10^{-1})$ was approximately 50, whereas, $\psi(10^3)$ was approximately 150 in the cell volume. (*B*, C) The schematic representation of the relationship between Amp_{PF} and Ca^* in the spine volume (*B*) and in the cell volume (C*)*. (*D*) The STD of Amp_{PF} dependency Amp^*, Amp_{PF} providing the maximum mutual information. (*E–X*) The Amp_{PF} dependencies of ΔCa^*_{STD}, the dynamic range of the distribution of Ca_{res} for $Ca_{res} > \theta$, (*green*) and σ_c, the standard deviation of the distribution of Ca_{res} (*blue*). The volume and STD are indicated.

Supporting Material Tables

Table S1. Parameters of the simple stochastic model in this study.

Parameters	Values
τ_{PF} [msec]	120
τ_{CF} [msec]	10
τ_{FB} [msec]	80
$Amp_{G_{IP_3R}}$	1291.6667
k [1/μm^3]	626.3027
K [1/μm^3]	626.3027
n_{IP_3R}	2.7
C_b [1/μm^3]	25.052108
V [μm^3]	10^{-1}–10^3

Table S2. Parameters that are different between the cases with various PF- and CF-timing and with single PF input alone.

Parameters	Values	
	PF and CF input (Figs. 1 and 2)	PF input alone (Figs. 3, 4, 5, and 6)
Amp_{CF} [1/μm^3]	361.328	None
Amp_{PF} [1/μm^3]	30.11×5 times	Variable×1 time
t_{CF} [msec]	variable	None
t_{PF} [msec]	{0, 10, 20, 30,40}	0
CV of PF input	Variable	0 (in simulation)

Note that the simple deterministic model shows the same results as those of the detailed deterministic model; however, with reduction of the model, the PF and CF inputs were non-dimensional values. With the loss of the dimension of the number of molecules, we could not perform the stochastic simulation. Therefore, we re-determined the numbers of PF and CF inputs as follows: The PF input becomes smaller than 1 in the spine volume (10^{-1} μm^3), but the PF input needs to be the positive integer. We increased the PF input 6-fold of the simple deterministic model so that the amount of IP_3, the mediator of PF input, is the same as that of the detailed stochastic model, resulting in the amplitude of a PF input in the spine volume of 3 ($Amp_{PF} \times V = 30.11 \times 10^{-1} = 3.011 \simeq 3$). We reduced the reaction rate constant of the Ca^{2+} release by binding IP_3 and IP_3R to one sixth to compensate for Ca_{IP_3}. The CF input increased 6-fold so that the amount of Ca^{2+} via the CF input in the simple stochastic model became the same as that in the detailed stochastic model.

Supporting Material Text

Derivation: The necessary and sufficient condition for robustness is satisfied when $\Delta Ca^* \ll \sigma_c$

We tried to examine the upper bound of the range of x where Eq. 21 in the main text is satisfied and showed that the upper bound of the range of x in the spine volume is larger than that in the cell volume. Hereafter, each distribution of Ca_{res} for $Ca_{res} > \theta$ and $Ca_{res} \leq \theta$ is approximated by the Gaussian distribution. We examined Eq. 21 in the main text as satisfied when σ_c, the standard deviation of Ca_{res}, is larger than ΔCa^*, the gap of the gap of the mode of the distribution of Ca_{res}, with $Amp_{PF} = \mu_a + x$ and $Amp_{PF} = \mu_a - x$. Here, we considered the small gap of Amp'_{PF}, therefore, for simplicity, $\sigma_c(\mu_a + x)$ and $\sigma_c(\mu_a - x)$, the standard deviations of Ca_{res} with $Amp_{PF} = \mu_a + x$ and $Amp_{PF} = \mu_a - x$, were regarded as $\sigma_c(\mu_a)$, the standard deviation of Ca_{res} with $Amp_{PF} = \mu_a$, up to the upper bound of the range of x satisfying Eq. 21 in the main text (see Fig. S5*A*, *B* in the Supporting Material).

First, we considered $p_c(Ca_{res}|Ca_{res} > \theta, \mu_a + x)$, the distribution of Ca_{res}, for $Ca_{res} > \theta$ in the spine and cell volumes and we approximated the distribution of Ca_{res} for $Ca_{res} > \theta$ by the Gaussian distribution, given by

$$p_c(Ca_{res}|Ca_{res} > \theta, \mu_a + x) \simeq \frac{1}{\sqrt{2\pi{\sigma_c}^2}} \exp\left[-\frac{\left(Ca_{res} - Ca^*(\mu_a + x)\right)^2}{2{\sigma_c}^2}\right]. \tag{S1}$$

Ca^* indicates the mode of the distribution of Ca_{res}, given by

$$Ca^*(a) = \arg\max_{Ca_{res}} p_c(Ca_{res}|Ca_{res} > \theta, a). \tag{S2}$$

As mentioned, we assumed $\sigma_c \equiv \sigma_c(\mu_a \pm x) = \sigma_c(\mu_a)$.

Then, for $Ca_{res} > \theta$, we substituted Eqs. 26 in the main text and S1 in right side of Eq. 25 in the main text, and obtained

$$\frac{1}{2}[p_c(Ca_{res}|\mu_a + x) + p_c(Ca_{res}|\mu_a - x)]$$

$$\simeq \frac{1}{2}\left\{\frac{P_+(\mu_a + x)}{\sqrt{2\pi{\sigma_c}^2}}\exp\left[-\frac{\left(Ca_{res} - Ca^*(\mu_a + x)\right)^2}{2{\sigma_c}^2}\right]\right.$$

$$\left. + \frac{P_+(\mu_a - x)}{\sqrt{2\pi{\sigma_c}^2}}\exp\left[-\frac{\left(Ca_{res} - Ca^*(\mu_a - x)\right)^2}{2{\sigma_c}^2}\right]\right\}. \quad \text{(S3)}$$

Here, we considered Ca^*. Ca^* for $Ca_{res} > \theta$ linearly increased from approximately $Amp_{PF} = 50$ in the spine volume (Fig. 4*A*, black line). In the spine volume, Ca^* for $Ca_{res} > \theta$ linearly increased with the increase in Amp_{PF} for $150 \leq Amp_{PF} \leq 215$, which corresponds to the range of the PF-CF input timing. Thus, regarding Ca^* for $Ca_{res} > \theta$, we could assume

$$Ca^*(\mu_a \pm x) \simeq Ca^*(\mu_a) \pm \Delta Ca^*(x). \quad \text{(S4)}$$

Equation S4 indicates that the difference of Ca^* with $Amp_{PF} = \mu_a + x$ and with $Amp_{PF} = \mu_a$ is the same as that with $Amp_{PF} = \mu_a$ and with $Amp_{PF} = \mu_a - x$, where ΔCa^* indicates the difference of Ca^* with $Amp_{PF} = \mu_a \pm x$ and with $Amp_{PF} = \mu_a$. In contrast to the spine volume, in the cell volume, Ca^* abruptly increased at $Amp_{PF} = 150$, and gradually increased with the increase in Amp_{PF} (Fig. S5*C* in the Supporting Material, yellow line). Therefore, in the cell volume, Eq. S4 is not satisfied at $Amp_{PF} = 150$, but it is almost satisfied for $150 < Amp_{PF} \leq 215$. Then, we substituted Eq. S4 in the Eq. S3, and obtained

$$\simeq \frac{1}{2}\left\{\frac{P_+(\mu_a+x)}{\sqrt{2\pi{\sigma_c}^2}}\exp\left[-\frac{\left(Ca_{res}-Ca^*(\mu_a)-\Delta Ca^*(x)\right)^2}{2{\sigma_c}^2}\right]\right.$$

$$\left.+\frac{P_+(\mu_a-x)}{\sqrt{2\pi{\sigma_c}^2}}\exp\left[-\frac{\left(Ca_{res}-Ca^*(\mu_a)+\Delta Ca^*(x)\right)^2}{2{\sigma_c}^2}\right]\right\}$$

$$=\frac{1}{2\sqrt{2\pi{\sigma_c}^2}}\exp\left[-\frac{\left(Ca_{res}-Ca^*(\mu_a)\right)^2}{2{\sigma_c}^2}\right]\exp\left[-\frac{\Delta Ca^*(x)^2}{2{\sigma_c}^2}\right]$$

$$\times\left\{P_+(\mu_a+x)\exp\left[\frac{\left(Ca_{res}-Ca^*(\mu_a)\right)\Delta Ca^*(x)}{{\sigma_c}^2}\right]\right.$$

$$\left.+P_+(\mu_a-x)\exp\left[-\frac{\left(Ca_{res}-Ca^*(\mu_a)\right)\Delta Ca^*(x)}{{\sigma_c}^2}\right]\right\}. \quad \text{(S5)}$$

Here, we considered the range of Ca_{res} where $|Ca_{res}-Ca^*(x)|\leq 3\sigma_c(x)$ is almost satisfied. Hence, if $\Delta Ca^*(x)\ll\sigma_c(x)$, then, we could approximate

$$\simeq\frac{1}{\sqrt{2\pi{\sigma_c}^2}}\exp\left[-\frac{\left(Ca_{res}-Ca^*(\mu_a)\right)^2}{2{\sigma_c}^2}\right]\left\{\frac{P_+(\mu_a+x)+P_+(\mu_a-x)}{2}\right\}. \quad \text{(S6)}$$

Note that, the upper bound of the range of x where $\Delta Ca^*\ll\sigma_c$ determines the upper bound of the range where Eq. 21 in the main text is satisfied. This means that the larger upper bound of the range of x where $\Delta Ca^*\ll\sigma_c$ corresponds to the maximum of CV_a with which the distribution of Ca_{res} does not change.

Here, we considered the probability that Ca_{res} exceeds the threshold θ, P_+. In the spine volume, P_+ gradually increased from $Amp_{PF}=50$ and linearly increased for $100\leq Amp_{PF}\leq 250$ (Fig. S5*D* in the Supporting Material, black line). Therefore, in the spine volume, P_+ linearly increased with the increase in Amp_{PF} for $150\leq Amp_{PF}\leq 215$, which corresponds to the range of the PF-CF input timing. Thus, regarding P_+, we could assume

$$\frac{1}{2}[P_+(\mu_a+x)+P_+(\mu_a-x)]=P_+(\mu_a). \quad \text{(S7)}$$

This equation indicates that the average of the probabilities that Ca_{res} exceeds the threshold θ with $Amp_{PF} = \mu_a + x$ and $Amp_{PF} = \mu_a - x$ is the same as the probability that Ca_{res} exceeds the threshold θ with $Amp_{PF} = \mu_a$. In the cell volume, the distribution of Ca_{res} was unimodal, and $\theta = -\infty$ was assumed; therefore, P_+ was always 1 and Eq. S7 was always satisfied. Therefore, we substituted Eq. S7 in the Eq. S6 and obtained

$$\frac{1}{2}[p_c(Ca_{res}|\mu_a + x) + p_c(Ca_{res}|\mu_a - x)] \simeq \frac{P_+(\mu_a)}{\sqrt{2\pi{\sigma_c}^2}} \exp\left[-\frac{\left(Ca_{res} - Ca^*(\mu_a)\right)^2}{2{\sigma_c}^2}\right]$$

$$= p_c(Ca_{res}|\mu_a) \tag{S8}$$

for $Ca_{res} > \theta$, *i.e.*, Eq. 21 in the main text for $Ca_{res} > \theta$ is satisfied.

However, for $Ca_{res} \leq \theta$, because Ca^* for $Ca_{res} \leq \theta$ was almost constant, the distribution Ca_{res} was mainly characterized only by P_- of the distribution of Ca_{res}, indicating

$$p_c(Ca_{res}|Ca_{res} \leq \theta, \mu_a) = p_c(Ca_{res}|Ca_{res} \leq \theta, \mu_a \pm x). \tag{S9}$$

Then, using Eq. 21 in the main text for $Ca_{res} \leq \theta$, similar to the case for $Ca_{res} > \theta$, we obtained

$$\begin{aligned}
&\frac{1}{2}[p_c(Ca_{res}|\mu_a + x) + p_c(Ca_{res}|\mu_a - x)] \\
&\simeq \frac{1}{2}[P_-(\mu_a + x)p_c(Ca_{res}|Ca_{res} \leq \theta, \mu_a + x) \\
&\qquad + P_-(\mu_a - x)p_c(Ca_{res}|Ca_{res} \leq \theta, \mu_a - x)] \\
&= \frac{1}{2}[P_-(\mu_a + x)p_c(Ca_{res}|Ca_{res} \leq \theta, \mu_a) + P_-(\mu_a - x)p_c(Ca_{res}|Ca_{res} \leq \theta, \mu_a)] \\
&\simeq \frac{1}{2}[P_-(\mu_a + x) + P_-(\mu_a - x)]p_c(Ca_{res}|Ca_{res} \leq \theta, \mu_a) \\
&= P_-(\mu_a)p_c(Ca_{res}|Ca_{res} \leq \theta, \mu_a) = p_c(Ca_{res}|\mu_a)
\end{aligned} \tag{S10}$$

for $Ca_{res} \leq \theta$, *i.e.*, Eq. 21 in the main text for $Ca_{res} \leq \theta$ is also satisfied. Therefore, from Eqs. S8 and S10, we derived Eq. 21 in the main text. Thus, we approximately showed that if Ca^* and P_+ linearly

increase with the increase in Amp_{PF} and $\Delta Ca^* \ll \sigma_c$, then Eq. 21 in the main text was satisfied. This means that the necessary and sufficient condition for robustness is satisfied in the range where the intrinsic noise, σ_c, is larger than the extrinsic noise, ΔCa^*.